

Osteopontin Is a Critical Inhibitor of Calcium Oxalate Crystal Formation and Retention in Renal Tubules

JEFFREY A. WESSON,* RICHARD J. JOHNSON,[§] MARRILDA MAZZALI,[†]
ANNE M. BESHENSKY,* SUSAN STIETZ,[†] CECI GIACHELLI,[†] LUCY LIAW,[†]
CHARLES E. ALPERS,[†] WILLIAM G. COUSER,[†] JACK G. KLEINMAN,* and
JEREMY HUGHES[†]

*Department of Veterans Affairs Medical Center and Medical College of Wisconsin, Milwaukee, Wisconsin;

[†]University of Washington, Seattle, Washington; [‡]Maine Medical Center Research Institute, University of

Maine, Maine; [§]Baylor College of Medicine, Houston, Texas.

Abstract. Calcium nephrolithiasis is the most common form of renal stone disease, with calcium oxalate (CaOx) being the predominant constituent of renal stones. Current *in vitro* evidence implicates osteopontin (OPN) as one of several macromolecular inhibitors of urinary crystallization with potentially important actions at several stages of CaOx crystal formation and retention. To determine the importance of OPN *in vivo*, hyperoxaluria was induced in mice targeted for the deletion of the OPN gene together with wild-type control mice. Both groups were given 1% ethylene glycol, an oxalate precursor, in their drinking water for up to 4 wk. At 4 wk, OPN-deficient

mice demonstrated significant intratubular deposits of CaOx crystals, whereas wild-type mice were completely unaffected. Retained crystals in tissue sections were positively identified as CaOx monohydrate by both polarized optical microscopy and x-ray powder diffraction analysis. Furthermore, hyperoxaluria in the OPN wild-type mice was associated with a significant 2- to 4-fold upregulation of renal OPN expression by immunocytochemistry, lending further support to a renoprotective role for OPN. These data indicate that OPN plays a critical renoprotective role *in vivo* as an inhibitor of CaOx crystal formation and retention in renal tubules. *jeremy.hughes@ed.ac.uk*

Renal stone disease or nephrolithiasis is a common clinical disorder, and calcium oxalate (CaOx) is the principal crystalline component in approximately 75% of all renal stones. Normal urine inhibits all aspects of CaOx crystal formation *in vitro*, and several studies support the hypothesis that defective inhibition of urinary crystallization may be of critical importance in determining individual susceptibility to stone formation (1–4). However, other studies have failed to demonstrate differences in urinary macromolecules between stone formers and controls (5–7). Several candidate inhibitory macromolecules have been isolated and identified in both urine and kidney stones, including osteopontin (OPN), nephrocalcin, crystal matrix protein, bikunin, and Tamm-Horsfall protein (8–12). *In vitro* data suggest that OPN may provide much of the inhibition of kidney stone formation observed in normal urine (13,17).

The multifunctional protein OPN is secreted by varied cell types and is involved in diverse biologic processes, including

inflammation, leukocyte recruitment, wound healing, and cell survival (14–18). OPN is also involved in biologic calcification, with osteoclast-derived OPN acting to inhibit hydroxyapatite formation during normal bone mineralization (19). In addition, macrophage and smooth muscle cell–derived OPN is associated with dystrophic calcification in degenerative and atheromatous vascular disease, with *in vitro* data suggesting an inhibitory action on such calcification (20–23). OPN is synthesized within the kidney (24) and is present in human urine at levels that can effectively inhibit CaOx crystallization (13,25). Indeed, reduced concentrations of OPN have been documented in urine from patients with renal stone disease compared with normal individuals (2,26). *In vitro* data indicate that urinary OPN may inhibit the nucleation, growth, and aggregation of CaOx crystals and directly inhibits the binding of CaOx crystals to cultured renal epithelial cells (8,27,28). OPN also directs CaOx crystallization to the CaOx dihydrate (COD) phase, which is significantly less adherent to renal tubular epithelial cells than the CaOx monohydrate (COM) phase (29). On the other hand, some have proposed a role for OPN as a promoter of stone formation, possibly acting to support tethering of CaOx crystals and tubular cell membranes (30,31).

Despite these numerous *in vitro* studies, there are no data currently available to indicate whether OPN or any of the other individual urinary macromolecules are critically required to prevent or promote stone formation *in vivo*. In this study, we tested the hypothesis that OPN is required for the effective inhibition of renal CaOx crystal formation and retention *in vivo*

Received October 11, 2002. Accepted September 3, 2002.

Dr. Jared J. Grantham served as Guest Editor and supervised the review and final disposition of this manuscript.

Correspondence to Dr. Jeremy Hughes, Phagocyte Laboratory, MRC Center for Inflammation Research, University of Edinburgh Medical School, Teviot Place, Edinburgh, EH8 9AG, United Kingdom. Phone: 44-131-6511574; Fax: 44-131-6511607; E-mail: jeremy.hughes@ed.ac.uk

1046-6673/1401-0139

Journal of the American Society of Nephrology

Copyright © 2002 by the American Society of Nephrology

DOI: 10.1097/01.ASN.0000040593.93815.9D

by inducing hyperoxaluria for up to 4 wk in both mice genetically targeted for the deletion of the OPN gene and wild-type, control mice. We also characterized the nature of the intrarenal CaOx crystals to further investigate the mechanism of action of OPN *in vivo*.

Materials and Methods

Experimental Animals

Deletion of the OPN gene was performed by targeted disruption as described previously (16). Briefly, the OPN gene was deleted through homologous recombination. Homozygous null mutant (knockout) mice were viable and fertile and breeding pairs of a Black Swiss genetic background were established to produce the animals used in this study. Wild-type breeding pairs of the same genetic background were used as controls. The genotype of animals was confirmed by PCR analysis. Previous studies have indicated that OPN knockout mice exhibit normal kidney architecture and renal function unless exposed to overt renal injury (17,32).

Experimental Model of Hyperoxaluria

Hyperoxaluria was induced in adult male OPN knockout and wild-type mice by the administration of 1% ethylene glycol (Sigma, St. Louis, MO), an oxalate precursor, in the drinking water. Twenty-four-hour urine collection was performed at baseline and at the 2 and 4 wk time points. The urine was characterized for relevant biochemical parameters as described below. Mice were sacrificed after 2 or 4 wk ($n = 6$ per group). Mice were injected with bromodeoxyuridine (BrdU) intraperitoneally 4 h before sacrifice (Cell proliferation kit, Amersham Pharmacia Biotech, Bucks, UK, 1 ml/100 g body weight). The kidneys were removed, cut longitudinally, fixed in either 10% buffered formalin or methyl Carnoy solution (60% methanol, 30% chloroform, and 10% acetic acid) and embedded in paraffin. Control kidney tissue was derived from age- and sex-matched non-manipulated OPN knockout and wild-type mice. A serum specimen was obtained at baseline and at 4 wk for biochemical analysis. Samples were frozen at -70°C until analysis. These studies were performed in an accredited animal care facility in accordance with the NIH guidelines for the care and use of laboratory animals.

Analysis of Serum and Urine

The concentrations of calcium and phosphate in serum and urine were determined by a Cobas autoanalyzer. Urine citrate and oxalate concentrations were determined by enzymatic colorimetric kits (Sigma). Urine samples were thawed and centrifuged at $17,000 \times g$ to sediment urine crystals. Urine crystal morphology was examined by both optical and polarized light microscopy. Urine crystals were also analyzed by x-ray powder diffraction at the VA National Crystal Identification Facility in Milwaukee, WI, through the kind assistance of Kathy Fryjoff and Dr. Neil Mandel. Some samples contained insufficient crystalline material to facilitate x-ray powder diffraction analysis on this equipment.

Detection of Renal Deposits of Calcium Oxalate and Crystal Identification Studies

Intrarenal deposits of CaOx were detected by von Kossa staining (33). Briefly, deparaffinized formalin-fixed 4- μm tissue sections were incubated in 5% silver nitrate for 60 min with exposure to ultraviolet light. Slides were rinsed in water, incubated in 5% sodium thiosulfate for 2 to 3 min, washed, and counterstained. Quantification of CaOx

crystal formation and retention was performed by counting the number of CaOx deposits per sagittal kidney section.

Visual characterization of retained crystals was performed by polarized light microscopy of hematoxylin and eosin-stained sections. Crystal composition was verified using a Bruker microdiffractometer in the IT Characterization Facility at the University of Minnesota, Minneapolis. Sections of renal tissue from three OPN knockout mice and one control OPN wild-type mouse (4 wk time point) were scraped off the microscope slide and mounted in the diffractometer, thereby enabling x-ray powder diffraction analysis to be performed on each entire tissue section.

Renal Morphology and Immunohistochemistry

Immunoperoxidase staining for OPN was performed on methyl Carnoy-fixed tissue. Four-micrometer sections were incubated with a goat polyclonal antibody against OPN at 4°C overnight followed by a biotinylated rabbit anti-goat IgG (Jackson Immuno-Research Laboratories, Inc., West Grove, PA) at room temperature for 30 min (17). Following incubation with horseradish peroxidase-conjugated avidin D (Vector Laboratories, Burlingame, CA) at room temperature for 20 min, brown staining was developed using diaminobenzidine (Sigma) without nickel as the chromogen, and slides were counterstained with methyl green. An irrelevant primary antibody of the same isotype was used as negative control. The percent area of OPN expression was determined using Optimas 6.2 computerized image analysis software (Optimas, v 6.2; Media Cybernetics, Silver Spring, MD) (17).

To identify and accurately quantify proximal and distal tubular epithelial cell proliferation and apoptosis, Fx1A/BrdU and Fx1A/TUNEL double-labeling was performed on formalin-fixed tissue sections as described previously (34). The Fx1A antibody, raised against rat proximal tubular brush border antigen, specifically stains the brush border of proximal tubular epithelial cells (35). Sections were incubated with biotinylated sheep Fx1A antibody at 4°C overnight, followed by horseradish peroxidase-conjugated avidin D (Vector Laboratories) for 20 min at room temperature. Staining was developed using DAB without nickel to produce a brown color. BrdU or TUNEL staining was then performed as indicated below using DAB with nickel as the chromogen.

Tissue sections were incubated with a murine IgG2a monoclonal antibody against BrdU (Cell proliferation kit; Amersham Pharmacia Biotech, Bucks, UK) at room temperature for 60 min, followed by a peroxidase-conjugated goat anti-mouse IgG2a (Cell proliferation kit; Amersham Pharmacia Biotech, Bucks, UK) at room temperature for 30 min. Before incubation with these antibodies, the tissue sections underwent an antigen retrieval step by boiling in 0.01 M sodium citrate buffer for a total of 10 min. After incubation with horseradish peroxidase-conjugated avidin D (Vector Laboratories) at room temperature for 20 min, black staining was developed using diaminobenzidine (Sigma) with nickel as the chromogen, and slides were counterstained with methyl green. An irrelevant primary antibody of the same isotype was used as negative control.

Apoptotic cells were detected by the TUNEL assay as described previously (36). Briefly, tissue sections underwent an antigen retrieval step by boiling in 0.01 M sodium citrate buffer for 2 min. Sections were then incubated with proteinase K (6.2 $\mu\text{g}/\text{ml}$; Boehringer Mannheim, Indianapolis, IN) followed by TdT (300 enzyme units/ml; Pharmacia Biotech, Piscataway, NJ) and Bio-14-dATP (0.94 nM; Life Technologies BRL, Grand Island, NY). Biotinylated ATP was detected using the ABC staining method (Vector Laboratories; following the manufacturer's protocol). As a positive control, slides were pretreated with DNAase (20 Kunitz units/ml; Sigma Biosciences, St Louis, MO).

The number of Fx1A⁺/BrdU⁺, Fx1A⁻/BrdU⁺, Fx1A⁺/TUNEL⁺, and Fx1A⁻/TUNEL⁺ cells in each biopsy was calculated in a blinded fashion by counting 20 sequentially selected fields at $\times 250$ magnification and expressed as the mean number \pm SEM per high power field (hpf) (34).

Statistical Analyses

Values are expressed as mean \pm SEM. Statistical significance, defined as $P < 0.05$, was evaluated using the *t* test.

Results

OPN Knockout and Wild-Type Mice Exhibit Comparable Serum and Urine Biochemistry

Twenty-four-hour fluid intake, 24-h urine volume, urine osmolality, and urine pH were comparable between OPN wild-type and knockout mice (data not shown), suggesting that renal handling of water together with urine acidification did not differ between genotypes. No significant differences were detected in serum and urine biochemistry between OPN knockout and wild-type mice, with the exception that OPN knockout mice exhibited a significantly reduced urine phosphate concentration at baseline but not at the 2 or 4 wk time points (Table 1). Importantly, no differences in urinary levels of citrate, a low molecular weight inhibitor of urinary crystallization, were evident (Table 1). Also, both OPN knockout and wild-type mice exhibited comparable levels of hyperoxaluria following treatment with 1% ethylene glycol (Table 1).

Crystalluria

All urine samples from both OPN knockout and wild-type mice exhibited COD crystals. There was no difference in the incidence of COM crystalluria between genotypes. However, COM crystalluria increased following the induction of hyperoxaluria (data not shown). About one third of samples contained struvite crystals, identified by both morphology and x-ray diffraction, but this was independent of genotype or the presence of hyperoxaluria. Calcium phosphate crystals were not identified in any sample.

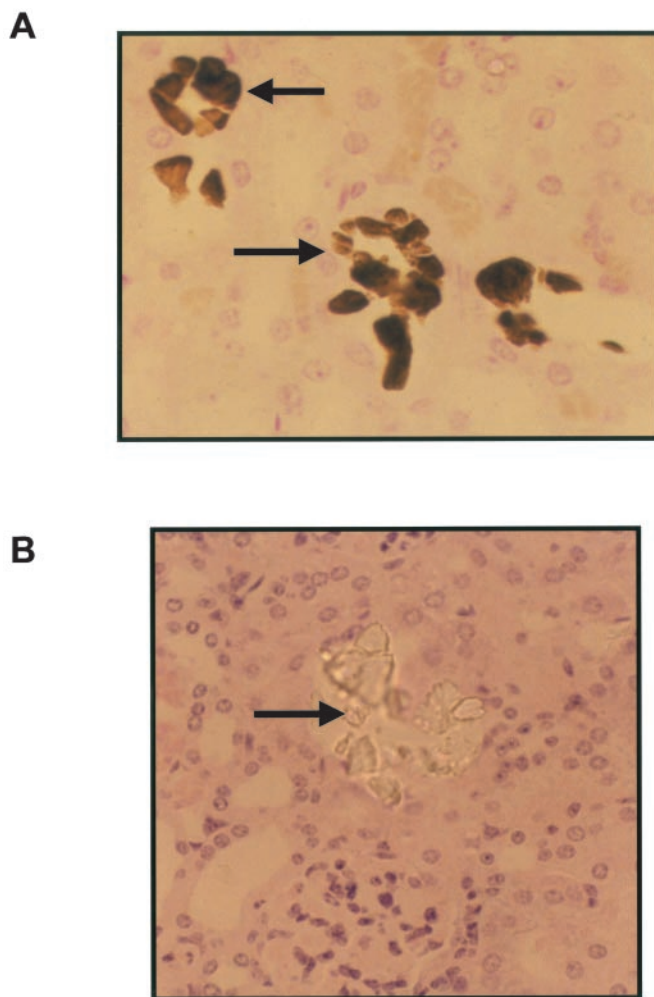


Figure 1. Photomicrograph of a kidney section from a hyperoxaluric osteopontin (OPN) knockout mouse (4 wk time point) stained with the von Kossa stain (magnification, $\times 630$) (A) or hematoxylin and eosin (B). Deposition of CaOx crystals (examples arrowed) occurs specifically within the tubular lumen (magnification, $\times 400$).

Table 1. Serum and urine biochemical analysis of serum and urine from osteopontin (OPN) knockout and wild-type mice

Parameter	Genotype	Baseline	2 wk	4 wk
Serum Ca ²⁺ (mg/dl)	KO	9.4 \pm 0.09	ND	9.5 \pm 0.13
Serum Ca ²⁺ (mg/dl)	WT	9.4 \pm 16	ND	9.8 \pm 0.15
Serum PO ₄ ²⁻ (mg/dl)	KO	7.2 \pm 0.36	ND	8.2 \pm 0.58
Serum PO ₄ ²⁻ (mg/dl)	WT	7.5 \pm 0.24	ND	7.7 \pm 0.49
Urine Ca ²⁺ (mg/dl)	KO	3.9 \pm 0.5	6.3 \pm 1.1	4.7 \pm 0.6
Urine Ca ²⁺ (mg/dl)	WT	6.3 \pm 1.1	4.8 \pm 0.6	5.2 \pm 0.9
Urine PO ₄ ²⁻ (mg/dl)	KO	180 \pm 26 ^a	182 \pm 51	280 \pm 33
Urine PO ₄ ²⁻ (mg/dl)	WT	329 \pm 30	253 \pm 49	294 \pm 42
Urinary citrate (mmol/L)	KO	4.4 \pm 1.7	3.7 \pm 1.6	5.2 \pm 2.3
Urinary citrate (mmol/L)	WT	4 \pm 1.1	2.5 \pm 0.9	2.1 \pm 1.4
Urinary oxalate (mg/L)	KO	38 \pm 8.9	169 \pm 29	308 \pm 78
Urinary oxalate (mg/L)	WT	56 \pm 13.8	149 \pm 55	285 \pm 58

^a $P < 0.05$ compared with OPN wild-type group at the same time point.

Table 2. Levels of proximal and distal tubular cell proliferation and apoptosis at 4 wk in osteopontin (OPN) knockout and wild-type (WT) mice^a

Parameter	OPN WT	OPN KO	P
BrDU-positive proximal tubular cells/10 hpf	6.55 ± 3.26	5.59 ± 2.06	0.8
BrDU-positive distal tubular cells/10 hpf	1.3 ± 0.55	1.31 ± 0.52	0.99
TUNEL-positive proximal tubular cells/10 hpf	0.55 ± 0.08	0.92 ± 0.61	0.6
TUNEL-positive distal tubular cells/10 hpf	0.3 ± 0.09	0.17 ± 0.08	0.288

^a Data are presented as mean ± SEM. hpf, high-power field.

Hyperoxaluric OPN Knockout Mice Develop Intratubular CaOx Crystal Formation and Retention

A period of 2 wk of treatment with 1% ethylene glycol did not induce detectable disease in either genotype despite the presence of significant levels of hyperoxaluria (Table 1). However, treatment for 4 wk with 1% ethylene glycol resulted in a further increase in urine oxalate concentrations (Table 1) and resulted in the development of intratubular CaOx crystal deposits in OPN knockout mice. CaOx crystals were evident in both von Kossa and hematoxylin and eosin–stained tissue sections (Fig 1). Crystal deposits were present in both the renal medulla and cortex and affected the distal nephron and collecting ducts. Quantification of crystal formation showed 14.3 ± 3 CaOx crystal inclusions per sagittal kidney section in OPN knockout mice with no CaOx deposits being found in OPN wild-type mice ($P < 0.02$).

Interestingly, there was no significant correlation between the urine oxalate concentration at 4 wk and the number of intratubular calcium oxalate crystals present in individual mice (data not shown).

Hyperoxaluric OPN Knockout and Wild-Type Mice Exhibit Comparable Levels of Tubular Cell Proliferation and Apoptosis

Our previous work indicated that OPN acts as a tubular epithelial cell survival factor *in vitro* and protects renal tubular epithelial cells from undergoing apoptosis *in vivo* during renal inflammation (17). It is therefore pertinent that CaOx may exhibit cytotoxicity to tubular epithelial cells (37), with proximal cells being more vulnerable to CaOx-mediated cell death than distal tubular cells (38). In addition, tubular cell injury has been documented to augment adhesion of CaOx crystals *in vitro* (39) as well as renal stone disease *in vivo* (40). We therefore examined the levels of proximal and distal tubular cell apoptosis (TUNEL) and proliferation (BrDU incorporation) following 4 wk of treatment with ethylene glycol, which resulted in the development of disease in OPN knockout mice. In contrast to previous work in rabbits (41), no significant differences between OPN wild-type and diseased OPN knockout mice were evident (Table 2), thereby suggesting that tubu-

lar cell injury was not a critical factor in the development of intratubular CaOx crystal formation in this study.

Crystal Deposits in Hyperoxaluric OPN Knockout Mice Were Calcium Oxalate Monohydrate

All crystals were located within the tubular lumen with no evidence of vascular, interstitial, or glomerular crystal deposition. Retained crystals were polycrystalline and could not be identified by conventional morphology in tissue sections. However, examination under polarizing optics demonstrated that the kidney sections from all OPN knockout mice contained strongly birefringent crystals, characteristic of COM or struvite (Figure 2). No non-birefringent or weakly birefringent crystals, suggestive of COD inclusions, were evident in tissue sections from any OPN knockout mice. In addition, x-ray powder diffraction analysis of entire tissue sections from 3 OPN knockout mice confirmed that the retained crystals were exclusively COM (Figure 3A), which is demonstrated by the presence of diffraction bands at characteristic positions for COM and the absence of bands for the other mineral phases. Renal tissue from an OPN wild-type mouse exhibited no diffraction bands characteristic of stone mineral crystals (Figure 3B), although strong bands characteristic of paraffin were observed in this sample due to incomplete removal of the embedding medium.

Absence of Disease in Hyperoxaluric OPN Wild-Type Mice Is Associated with Significant Upregulation of OPN Expression

OPN is usually expressed at a low level in normal renal tissue (32) (Figure 4A) but was markedly upregulated in wild-type mice following 4 wk of hyperoxaluria (Figure 4B). Quantification of OPN expression by computerized image analysis demonstrated significant upregulation of OPN expression in wild-type mice. OPN expression was increased approximately twofold in the renal cortex and fourfold in the renal medulla compared with untreated control wild-type mice (Figure 5). Upregulation of OPN expression was evident along the distal nephron and in the medullary collecting ducts.

Discussion

An accumulating body of data indicates that OPN is intimately involved in the regulation of both normal and pathologic mineralization. One of the most important forms of the latter found in clinical practice is renal stone disease. Many data support a role for OPN and other urinary macromolecules as inhibitors of the formation of insoluble calcium salts within urine (8–12,27). The proposed involvement of several macromolecular inhibitors suggests an element of redundancy, although to date there has been no study that attempts to isolate the action of any of these candidate crystallization inhibitors *in vivo*. We have also noted that some have proposed a role for OPN as a promoter of stone formation (30,31). The experiments reported above test both the importance of OPN in stone formation processes as well as its mode of action.

The first major finding of this study is that the induction of hyperoxaluria in OPN knockout mice exposes a significant

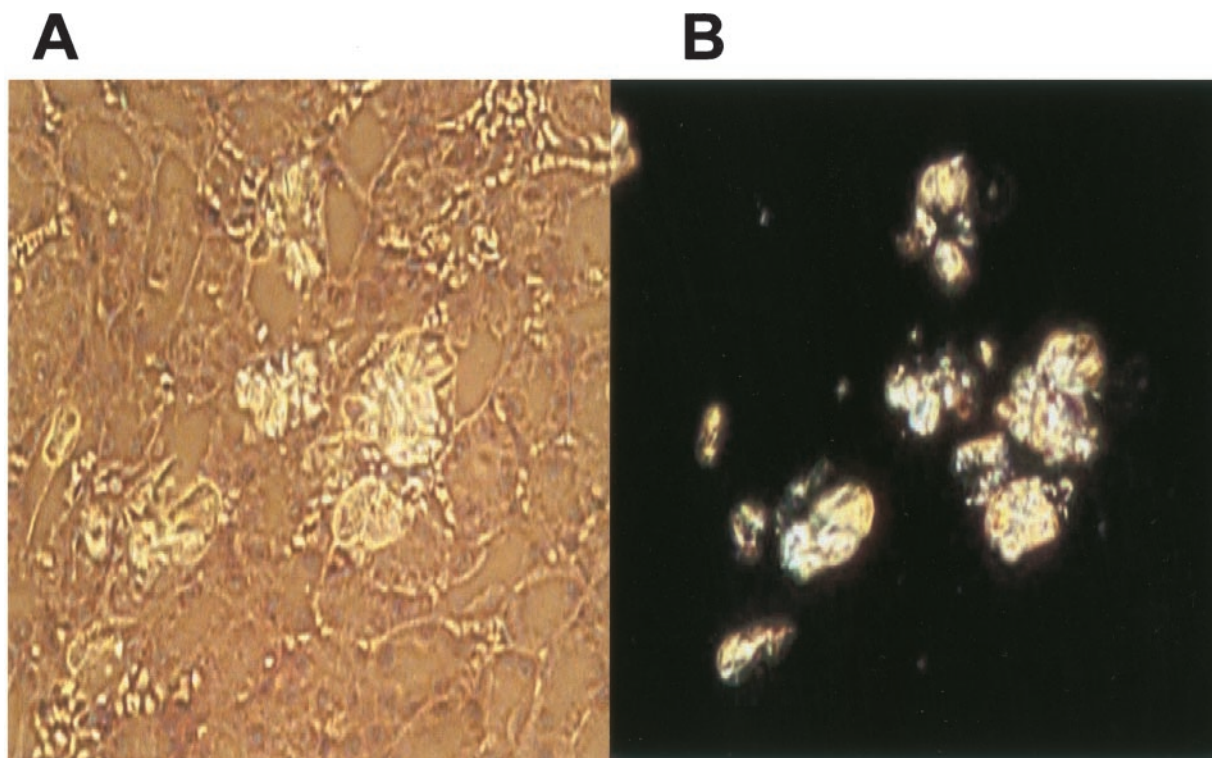


Figure 2. Photomicrograph of a kidney section from a hyperoxaluric OPN knockout mouse (4 wk time point). (A) Tissue section lightly stained with hematoxylin and eosin. (B) Polarized light optical photomicrograph of the same field at same magnification. Retained crystals exhibit strong birefringence.

functional defect in the ability of tubular fluid lacking OPN to adequately inhibit CaOx crystal formation and retention. Following 4 wk of hyperoxaluria, the OPN knockout mice developed significant renal CaOx crystal deposits and the wild-type mice were completely unaffected. CaOx crystals were found in the distal nephron and collecting duct, where the highest urinary concentration of oxalate would be predicted to occur as a consequence of homeostatic water conservation. Interestingly, the absence of disease at 2 wk indicates that OPN knockout mice are able to withstand a significant level of hyperoxaluria without developing disease. This is consistent with previously reported observations, where adding 1% ethylene glycol to drinking water failed to induce crystal formation and retention (42) (43). However, further elevation in urinary oxalate levels at 4 wk apparently exceeded the inhibitory capacity of OPN knockout urine, resulting in the formation and retention of CaOx crystals. Clearly, our data support an inhibitory role for OPN, with respect to crystal formation and retention, and therefore, stone disease.

CaOx crystal formation and retention occurred in the absence of any other significant differences between genotypes. In our measurements of pertinent serum and urine chemistries following induction of hyperoxaluria, the only significant difference observed was slightly diminished urinary phosphate levels in OPN knockout mice at baseline. However, this is likely to be inconsequential since there were no calcium phosphate crystals identified in any urine or tissue sample that could

serve as a nidus for subsequent CaOx crystallization. Indeed, the higher phosphate levels, and hence greater risk for crystallization, were found in wild-type mice, where no intratubular crystals were observed at any test condition. In our measurements of levels of tubular cell proliferation and apoptosis, no differences were seen between the genotypes. Although the OPN knockout mice were expected to be at higher risk for cell damage (17,37), the absence of measurable differences in apoptosis (TUNEL) and proliferation (BrDU) assays between the genotypes argues strongly against a significant role for cell damage in CaOx crystal deposition in the OPN knockout mice.

We are cognizant of the fact that experiments involving mice targeted for the deletion of various genes may be problematic due to alterations in expression of genes for other relevant proteins. One alternative is that deletion of the targeted gene may result in compensatory upregulation of other genes coding for proteins with related function. This alteration in the expression of other genes would minimize the biologic effect of the deletion and could lead to the absence of a discernible phenotype in the genetically manipulated animals. However, a clear phenotypic difference has been demonstrated in this study between the OPN-deficient mice and control animals. If other genes are upregulated after OPN deletion, it would further emphasize the importance of OPN in preventing stone formation. The other alternative is that deleting of the OPN gene may result in downregulation of other, potentially more significant inhibitors. Under this assumption, the phenotype (crystal dep-

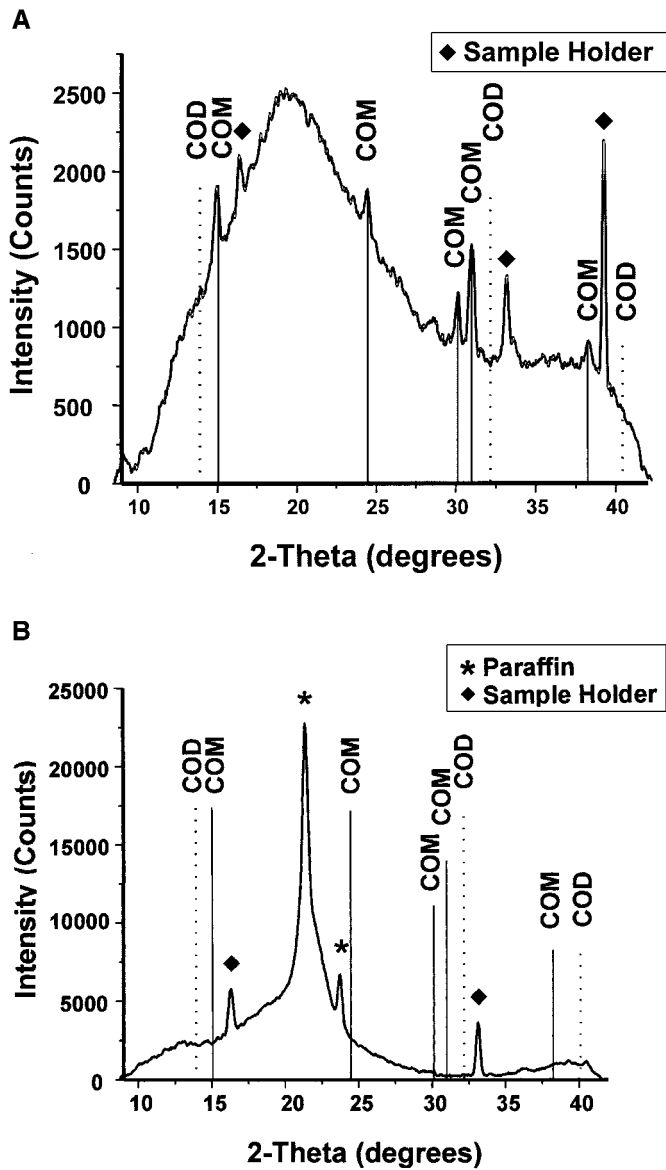


Figure 3. X-ray diffraction pattern of renal tissue from a hyperoxaluric OPN knockout (A) or wild-type (B) mouse (both at 4 wk time point). Positions of principal diffraction lines for CaOx monohydrate (COM; indicated by M designation) and CaOx dihydrate (COD; indicated by D designation) are shown in arbitrary units in each frame of this figure. The diffraction pattern from the OPN knockout mouse shows multiple diffraction peaks characteristic of COM and no peaks characteristic of COD or struvite. The OPN wild-type mouse sample exhibits no evidence of any stone crystal related bands. Paraffin bands appear as a result of incomplete removal of embedding medium. Note that the relative diffraction band intensities are not important in this analysis. The diffraction intensity is dependent on experimental conditions, including sample size, counting time, and sample orientation, whereas the diffraction band positions are characteristic of the particular crystalline materials present in the sample.

osition) would be enhanced by the genetic manipulation, although not directly as a result of OPN deletion. Although the levels of other candidate inhibitor macromolecules, such as

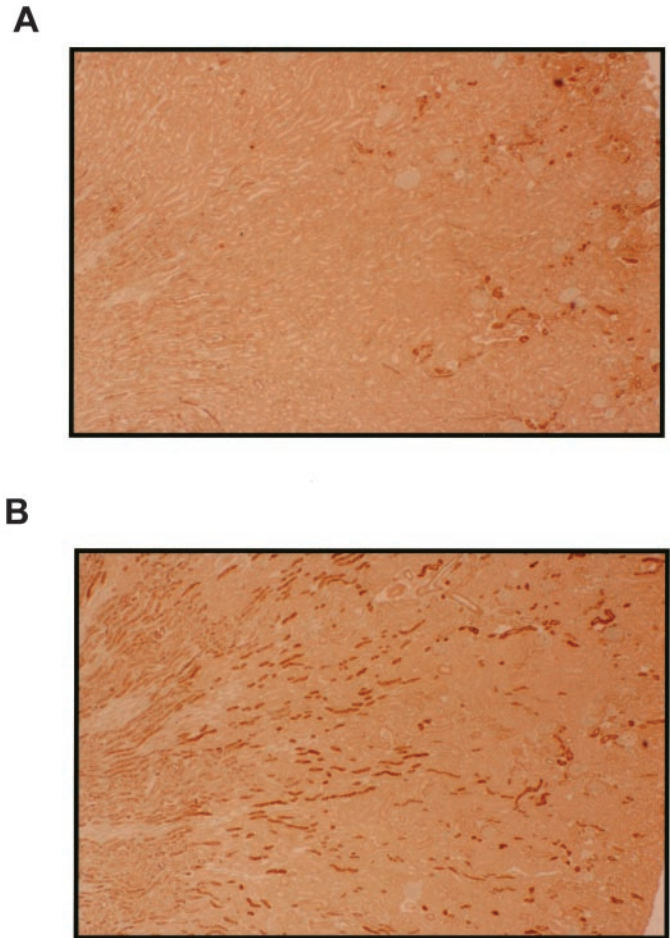


Figure 4. Immunocytochemical staining for OPN in (A) untreated OPN wild-type mice or (B) hyperoxaluric OPN wild-type mice (4 wk time point).

nephrocalcin or Tamm Horsfall protein, were not measured in this study, careful consideration of our observations argue against any significant reduction in their levels. As noted above, even the OPN-deficient mice were resistant to crystal formation and deposition even after 2 wk on an oxalate inducing diet, which suggests that these mice had other protective mechanisms against CaOx crystal deposition. We also note that the principal urinary crystals found in samples from both the wild-type and the genetically altered mice were COD, indicating the presence of soluble inhibitors in the urine from both genotypes. Although we are unable to categorically exclude a global downregulation of urinary tract CaOx crystallization inhibitors, we feel our data support the straightforward conclusion that OPN is a biologically important inhibitor of CaOx crystal formation and retention, and therefore, stone formation, although other components also play a role.

Previous work indicates that exposure to CaOx may result in tubular cell injury and that the deliberate induction of tubular cell injury aggravates CaOx crystal formation *in vivo* (37) (40). In addition, tubular cell apoptosis results in increased adhesion of CaOx crystals (37). In light of the fact that OPN is a documented tubular cell survival factor (17), it is possible that

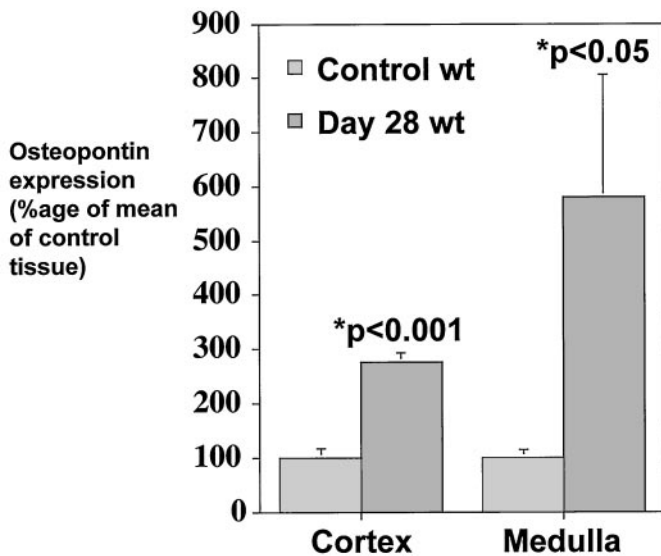


Figure 5. Quantification of OPN staining (4 wk time point) indicates significant upregulation of OPN expression after induction of hyperoxaluria.

OPN knockout mice in this study developed increased levels of tubular cell apoptosis and injury, which consequently increase CaOx crystal formation. However, we found no differences in the levels of tubular cell apoptosis and proliferation evident in OPN knockout and wild-type mice at the 4 wk time point, suggesting that differences in tubular cell injury between experimental groups was not a factor in the development of CaOx crystal deposits in this study.

The presence of struvite crystals in the urine of some mice appears to be completely unrelated to the presence or absence of CaOx crystal inclusions. Struvite crystals are associated with urinary tract infection in humans, but their significance in this study is unclear. Although struvite was found in urine samples from both genotypes under baseline or hyperoxaluric conditions, there was no evidence of struvite crystal formation and retention within renal tissue and no correlation between struvite crystalluria and any other experimental parameter.

The second major finding of this study was the observation that the CaOx deposits in OPN knockout mice were comprised exclusively of COM crystals. This observation reaffirms COM as the pathologic crystalline form of CaOx with respect to stone formation, supporting previous observations in human stone samples (44) and animal studies (45). Unfortunately, determination of the exact mechanism of renoprotection afforded by the presence of OPN in hyperoxaluric OPN wild-type mice in this study is complicated by the multiple actions of OPN (Figure 6). For example, OPN-mediated kinetic inhibition of CaOx crystallization (27) may sufficiently delay formation of COM crystals until they are beyond some critical point for attachment within the renal tubule. In addition, OPN may directly inhibit COM (or COD) crystal adhesion to tubular epithelial cells (46) or augment intratubular production of the less adhesive COD at the expense of COM (29). Indeed, it may be the case that the sum of these multiple actions is required for

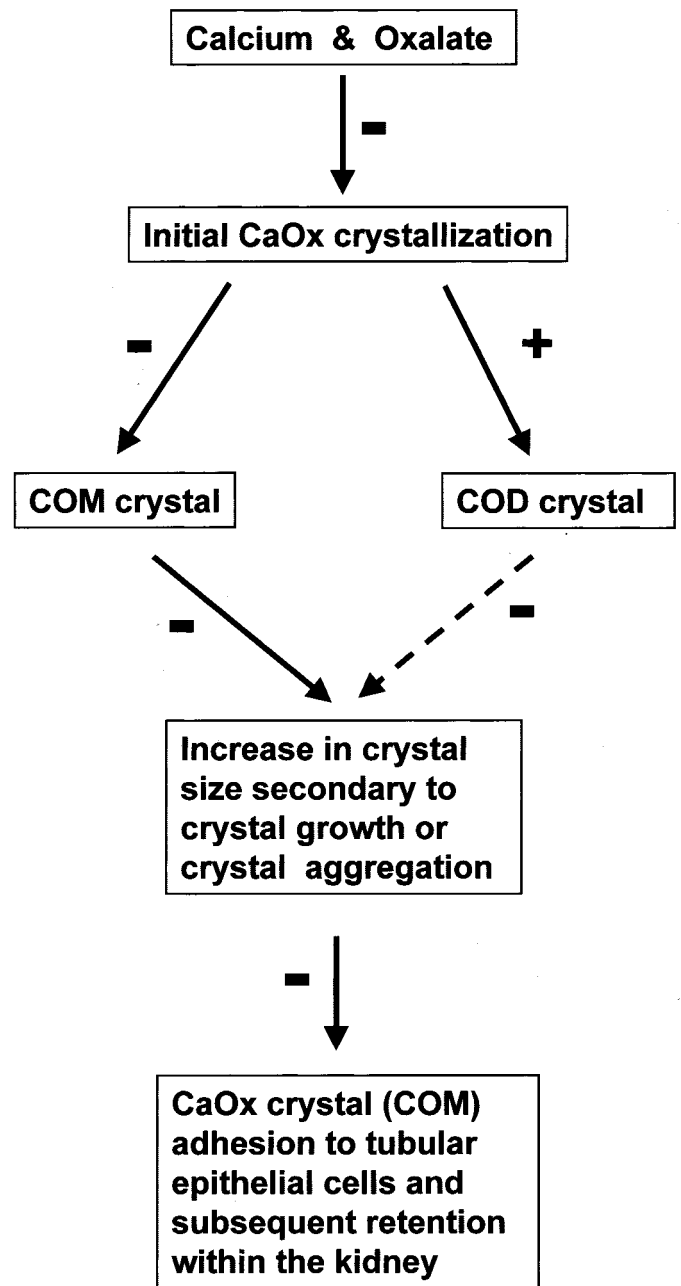


Figure 6. Hypothetical schema depicting the multiple actions of osteopontin that may be required to adequately inhibit the intrarenal deposition of calcium oxalate crystals (–, inhibited by osteopontin; +, favored by osteopontin).

effective inhibition of CaOx crystal formation by OPN. Resolution of these issues awaits the development of methods to accurately demonstrate and quantitate specific crystal phases of CaOx within the various nephron segments of hyperoxaluric OPN wild-type and knockout mice before the development of crystal deposits.

Examination of urinary crystals in this study was informative, although we are cognizant of the fact that they may not accurately reflect the crystals present within the tubular lumen *in vivo*. COD was the dominant CaOx crystal phase under

normal conditions in both genotypes, indicating that the presence of OPN is not essential for COD formation. This is not surprising; other urinary molecules can influence CaOx phase behavior *in vitro* (29). We did observe an increase in the degree of COM crystalluria after the induction of hyperoxaluria, although there were no significant differences between genotypes. This suggests that urinary crystallization inhibitors have a finite capacity to limit the production of potentially pathologic COM crystals by augmentation of COD crystal formation or other mechanisms.

Finally, the important role played by OPN is emphasized by the significant upregulation of both cortical and medullary OPN expression in hyperoxaluric OPN wild-type mice. This mirrors *in vitro* data indicating that cultured renal epithelial cells respond to CaOx crystal exposure by upregulating both OPN production and secretion (47). Before this study, the only available *in vivo* data regarding OPN expression in renal stone disease was from experiments involving hyperoxaluric rats, which develop renal CaOx deposits. In these studies, upregulation of OPN mRNA and protein expression specifically colocalized with areas of renal CaOx crystal formation, suggesting an important role for OPN (48,49), but these observations were unable to distinguish inhibition from promotion. Furthermore, we noted that upregulation of OPN expression in wild-type mice was mainly along the distal nephron and the medullary collecting ducts, which were the principal sites of intratubular CaOx crystal formation and retention in diseased OPN knockout mice.

In summary, hyperoxaluric OPN knockout mice developed significant renal tubular inclusions of COM, whereas OPN wild-type mice were completely protected. The marked upregulation of renal tubular OPN expression in disease-free hyperoxaluric OPN wild-type mice lends further support to a renoprotective role for OPN. These data indicate that OPN is a critical inhibitor of CaOx crystal formation and retention in the kidney *in vivo*. OPN is implicated in the pathogenesis of renal stone disease in humans (25,26); therefore, the future characterization of the molecular mechanism of action of OPN may well provide opportunities for the development of novel therapeutic drug treatments for renal stone disease.

Acknowledgments

JAW was supported by a VA Research Career Development grant (9305–01CD) and development funds from the Medical College of Wisconsin. RJJ was supported by a George O'Brien Center NIH grant DK-47659 and by NIH DK-52121. JGK was supported by NIH grant DK-48504. JH was a Wellcome Trust Advanced Fellow and is now in receipt of a Wellcome Trust Senior Research Fellowship in Clinical Science. We also express our gratitude to Dr. Neil Mandel and Kathy Fryjoff at the VA National Crystal Identification Facility, Milwaukee, Wisconsin, and to Linda Sauer at the IT Characterization Facility, University of Minnesota, Minneapolis, for their expertise and assistance in obtaining x-ray diffraction of various samples.

References

- Asplin JR, Parks JH, Chen MS, Lieske JC, Toback FG, Pillay SN, Nakagawa Y, Coe F: Reduced crystallization inhibition by urine from men with nephrolithiasis. *Kidney Int* 56: 1505–1516, 1999
- Nishio S, Hatanaka M, Takeda H, Aoki K, Iseda T, Iwata H, Yokoyama M: Calcium Phosphate Crystal-Associated Proteins: alpha2-HS-Glycoprotein, Prothrombin F1, and Osteopontin. *Mol Urol* 4: 383–390, 2000
- Glauser A, Hochreiter W, Jaeger P, Hess B: Determinants of urinary excretion of Tamm-Horsfall protein in non-selected kidney stone formers and healthy subjects. *Nephrol Dial Transplant* 15: 1580–1587, 2000
- Romero MC, Nocera S, Nesse AB: Decreased Tamm-Horsfall protein in lithiasic patients. *Clin Biochem* 30: 63–67, 1997
- Hedgepeth RC, Yang L, Resnick MI, Marengo SR: Expression of proteins that inhibit calcium oxalate crystallization *in vitro* in the urine of normal and stone-forming individuals. *Am J Kidney Dis* 37: 104–112, 2001
- Porile JL, Asplin JR, Parks JH, Nakagawa Y, Coe FL: Normal calcium oxalate crystal growth inhibition in severe calcium oxalate nephrolithiasis. *J Am Soc Nephrol* 7: 602–607, 1996
- Crassweller PO, Oreopoulos DG, Toguri A, Husdan H, Wilson DR, Rapoport A: Studies in inhibitors of calcification and levels of urine saturation with calcium salts in recurrent stone patients. *J Urol* 120: 6–10, 1978
- Shiraga H, Min W, VanDusen WJ, Clayman MD, Miner D, Terrell CH, Sherbotie JR, Foreman JW, Przysiecki C, Neilson EG, Hoyer JR: Inhibition of calcium oxalate crystal growth *in vitro* by uropontin: Another member of the aspartic acid-rich protein superfamily. *Proc Natl Acad Sci USA* 89: 426–430, 1992
- Coe FL, Nakagawa Y, Asplin J, Parks JH: Role of nephrocalcin in inhibition of calcium oxalate crystallization and nephrolithiasis. *Miner Electrolyte Metab* 20: 378–384, 1994
- Stapleton AM, Ryall RL: Crystal matrix protein—Getting blood out of a stone. *Miner Electrolyte Metab* 20: 399–409, 1994
- Atmani F, Khan SR: Role of urinary bikunin in the inhibition of calcium oxalate crystallization. *J Am Soc Nephrol* 10: S385–S388, 1999
- Hess B: Tamm-Horsfall glycoprotein and calcium nephrolithiasis. *Miner Electrolyte Metab* 20: 393–398, 1994
- Asplin JR, Arsenault D, Parks JH, Coe FL, Hoyer JR: Contribution of human uropontin to inhibition of calcium oxalate crystallization. *Kidney Int* 53: 194–199, 1998
- O'Brien ER, Garvin MR, Stewart DK, Hinohara T, Simpson JB, Schwartz SM, Giachelli CM: Osteopontin is synthesized by macrophage, smooth muscle, and endothelial cells in primary and restenotic human coronary atherosclerotic plaques. *Arterioscler Thromb* 14: 1648–1656, 1994
- Giachelli CM, Lombardi D, Johnson RJ, Murry CE, Almeida M: Evidence for a role of osteopontin in macrophage infiltration in response to pathological stimuli *in vivo*. *Am J Pathol* 152: 353–358, 1998
- Liaw L, Birk DE, Ballas CB, Whitsitt JS, Davidson JM, Hogan BL: Altered wound healing in mice lacking a functional osteopontin gene (*spp1*). *J Clin Invest* 101: 1468–1478, 1998
- Ophascharoensuk V, Giachelli CM, Gordon K, Hughes J, Pichler R, Brown P, Liaw L, Schmidt R, Shankland SJ, Alpers CE, Couser WG, Johnson RJ: Obstructive uropathy in the mouse: role of osteopontin in interstitial fibrosis and apoptosis. *Kidney Int* 56: 571–580, 1999
- Scatena M, Almeida M, Chaisson ML, Fausto N, Nicosia RF, Giachelli CM: NF-kappaB mediates alphavbeta3 integrin-induced endothelial cell survival. *J Cell Biol* 141: 1083–1093, 1998

19. Hunter GK, Kyle CL, Goldberg HA: Modulation of crystal formation by bone phosphoproteins: Structural specificity of the osteopontin-mediated inhibition of hydroxyapatite formation. *Biochem J* 300: 723–728, 1994
20. O'Brien KD, Kuusisto J, Reichenbach DD, Ferguson M, Giachelli C, Alpers CE, Otto CM: Osteopontin is expressed in human aortic valvular lesions. *Circulation* 92: 2163–2168, 1995
21. Srivatsa SS, Harrity PJ, Maercklein PB, Kleppe L, Veinot J, Edwards WD, Johnson CM, Fitzpatrick LA: Increased cellular expression of matrix proteins that regulate mineralization is associated with calcification of native human and porcine xenograft bioprosthetic heart valves. *J Clin Invest* 99: 996–1009, 1997
22. Ikeda T, Shirasawa T, Esaki Y, Yoshiki S, Hirokawa K: Osteopontin mRNA is expressed by smooth muscle-derived foam cells in human atherosclerotic lesions of the aorta. *J Clin Invest* 92: 2814–2820, 1993
23. Wada T, McKee MD, Steitz S, Giachelli CM: Calcification of vascular smooth muscle cell cultures: Inhibition by osteopontin. *Circ Res* 84: 166–178, 1999
24. Kleinman JG, Beshensky A, Worcester EM, Brown D: Expression of osteopontin, a urinary inhibitor of stone mineral crystal growth, in rat kidney. *Kidney Int* 47: 1585–1596, 1995
25. Min W, Shiraga H, Chalko C, Goldfarb S, Krishna GG, Hoyer JR: Quantitative studies of human urinary excretion of uropontin. *Kidney Int* 53: 189–193, 1998
26. Nishio S, Hatanaka M, Takeda H, Iseda T, Iwata H, Yokoyama M: Analysis of urinary concentrations of calcium phosphate crystal-associated proteins: alpha2-HS-glycoprotein, prothrombin F1, and osteopontin. *J Am Soc Nephrol* 10: S394–S396, 1999
27. Worcester EM, Beshensky AM: Osteopontin inhibits nucleation of calcium oxalate crystals. *Ann N Y Acad Sci* 760: 375–377, 1995
28. Lieske JC, Norris R, Toback FG: Adhesion of hydroxyapatite crystals to anionic sites on the surface of renal epithelial cells. *Am J Physiol* 273: F224–F233, 1997
29. Wesson JA, Worcester EM, Wiessner JH, Mandel NS, Kleinman JG: Control of calcium oxalate crystal structure and cell adherence by urinary macromolecules. *Kidney Int* 53: 952–957, 1998
30. Kohri K, Nomura S, Kitamura Y, Nagata T, Yoshioka K, Iguchi M, Yamate T, Umekawa T, Suzuki Y, Sinohara H: Structure and expression of the mRNA encoding urinary stone protein (osteopontin). *J Biol Chem* 268: 15180–15184, 1993
31. Yamate T, Kohri K, Umekawa T, Iguchi M, Kurita T: Osteopontin antisense oligonucleotide inhibits adhesion of calcium oxalate crystals in Madin-Darby canine kidney cell. *J Urol* 160: 1506–1512, 1998
32. Rittling SR, Denhardt DT: Osteopontin function in pathology: Lessons from osteopontin-deficient mice. *Exp Nephrol* 7: 103–113, 1999
33. Sheehan DC, Hrapchak BB: *Theory and Practice of Histotechnology*. St. Louis, Mosby, 1980, pp 227–228
34. Hughes J, Shankland SJ: Cyclin kinase inhibitor p21CIP1/WAF1 limits interstitial cell proliferation following ureteric obstruction. *Am J Physiol* 277: F948–F956, 1999
35. Edgington TS, Glasscock RJ, Dixon FJ: Autologous immune complex nephritis induced with renal tubular antigen. I. Identification and isolation of the pathogenetic antigen. *J Exp Med* 127: 555–572, 1968
36. Baker AJ, Mooney A, Hughes J, Lombardi D, Johnson RJ, Savill J: Mesangial cell apoptosis: The major mechanism for resolution of glomerular hypercellularity in experimental mesangial proliferative nephritis. *J Clin Invest* 94: 2105–2116, 1994
37. Wiessner JH, Hasegawa AT, Hung LY, Mandel NS: Oxalate-induced exposure of phosphatidylserine on the surface of renal epithelial cells in culture. *J Am Soc Nephrol* 10: S441–S445, 1999
38. Thamilselvan S, Hackett RL, Khan SR: Cells of proximal and distal tubular origin respond differently to challenges of oxalate and calcium oxalate crystals. *J Am Soc Nephrol* 10: S452–S456, 1999
39. Wiessner JH, Hasegawa AT, Hung LY, Mandel GS, Mandel NS: Mechanisms of calcium oxalate crystal attachment to injured renal collecting duct cells. *Kidney Int* 59: 637–644, 2001
40. Kumar S, Sigmon D, Miller T, Carpenter B, Khan S, Malhotra R, Scheid C, Menon M: A new model of nephrolithiasis involving tubular dysfunction/injury. *J Urol* 146: 1384–1389, 1991
41. Sarica K, Yagci F, Bakir K, Erbagci A, Erturhan S, Ucak R: Renal tubular injury induced by hyperoxaluria: Evaluation of apoptotic changes. *Urol Res* 29: 34–37, 2001
42. Lamb JC, Maronpot RR, Gulati DK, Russell VS, Hommel-Barnes L, Sabharwal PS: Reproductive and developmental toxicity of ethylene glycol in the mouse. *Toxicol Appl Pharmacol* 81: 100–112, 1985
43. Melnick RL: Toxicities of ethylene glycol and ethylene glycol monoethyl ether in Fischer 344/N rats and B6C3F1 mice. *Environ Health Perspect* 57: 147–155, 1984
44. Prien EL: Crystallographic analysis of urinary calculi: A 23 year study. *J Urol* 89: 917–924, 1963
45. Khan SR, Finlayson B, Hackett RL: Experimental calcium oxalate nephrolithiasis in the rat. *Role of the renal papilla*. *Am J Pathol* 107: 59–69, 1982
46. Lieske JC, Leonard R, Toback FG: Adhesion of calcium oxalate monohydrate crystals to renal epithelial cells is inhibited by specific anions. *Am J Physiol* 268: F604–F612, 1995
47. Lieske JC, Hammes MS, Hoyer JR, Toback FG: Renal cell osteopontin production is stimulated by calcium oxalate monohydrate crystals. *Kidney Int* 51: 679–686, 1997
48. Gokhale JA, Glenton PA, Khan SR: Localization of tamm-horsfall protein and osteopontin in a rat nephrolithiasis model. *Nephron* 73: 456–461, 1996
49. Jiang XJ, Feng T, Chang LS, Kong XT, Wang G, Zhang ZW, Guo YL: Expression of osteopontin mRNA in normal and stone-forming rat kidney. *Urol Res* 26: 389–394, 1998

**Access to UpToDate on-line is available for additional clinical information
at <http://www.jasn.org/>**